BBA - Bioenergetics 1859 (2018) 253–262

Contents lists available at ScienceDirect

BBA - Bioenergetics

journal homepage: www.elsevier.com/locate/bbabio

Rational redesign of the ferredoxin-NADP$^+$-oxido-reductase/ferredoxin-interaction for photosynthesis-dependent H_2-production

Wiegand K.[a,1], Winkler M.[b,1], Rumpel S.[c,1], Kannchen D.[a], Rexroth S.[a], Hase T.[d], Farès C.[e], Happe T.[b], Lubitz W.[c], Rögner M.[a,*]

[a] Plant Biochemistry, Faculty of Biology & Biotechnology, Ruhr University Bochum, 44780 Bochum, Germany
[b] Photobiotechnology, Faculty of Biology & Biotechnology, Ruhr University Bochum, 44780 Bochum, Germany
[c] Max-Planck-Institut für Chemische Energiekonversion, 45470 Mülheim, Germany
[d] Institute for Protein Research, Osaka University, Suita 565-0871, Osaka, Japan
[e] Max-Planck-Institut für Kohlenforschung, 45470 Mülheim, Germany

ARTICLE INFO

Keywords:
Protein design
Protein interaction
FNR
NMR
Photosynthesis
Synechocystis

ABSTRACT

Utilization of electrons from the photosynthetic water splitting reaction for the generation of biofuels, commodities as well as application in biotransformations requires a partial rerouting of the photosynthetic electron transport chain. Due to its rather negative redox potential and its bifurcational function, ferredoxin at the acceptor side of Photosystem 1 is one of the focal points for such an engineering. With hydrogen production as model system, we show here the impact and potential of redox partner design involving ferredoxin (Fd), ferredoxin-oxido-reductase (FNR) and [FeFe]-hydrogenase HydA1 on electron transport in a future cyanobacterial design cell of *Synechocystis* PCC 6803. X-ray-structure-based rational design and the allocation of specific interaction residues by NMR-analysis led to the construction of Fd- and FNR-mutants, which in appropriate combination enabled an about 18-fold enhanced electron flow from Fd to HydA1 (in competition with equimolar amounts of FNR) in *in vitro* assays. The negative impact of these mutations on the Fd-FNR electron transport which indirectly facilitates H_2 production (with a contribution of ≤42% by FNR variants and ≤23% by Fd-variants) and the direct positive impact on the Fd-HydA1 electron transport (≤23% by Fd-mutants) provide an excellent basis for the construction of a hydrogen-producing design cell and the study of photosynthetic efficiency-optimization with cyanobacteria.

1. Introduction

Cyanobacteria harvest light energy with particular efficiency and transform it into chemical energy - a process which goes along with CO_2-fixation and oxygen release. Due to the many steps involved in this process, the final efficiency of photosynthesis - based on the output of sugar or related compounds - is very low, routinely below 1% [1]. It is therefore tempting to modify the natural cyanobacterial metabolism to shorten the process of energy transformation as much as possible in order to increase the efficiency and to capture compounds suitable for long-term energy storage directly from photosynthesis. Hydrogen (H_2) fulfills these requirements and is one of the possible photosynthetic products of both, cyanobacteria [2] and green algae [3,4]. Besides its high energy content and unmatched environmental sustainability, H_2 is easily harvested due to its release from the cells into the medium. The S-deprivation metabolism of green algae like *Chlamydomonas reinhardtii* provides an impressive natural example for an enduring and productive photohydrogen evolution activity based on the [FeFe]-hydrogenase HydA1; remarkably, this enzyme is directly coupled to the photosynthetic electron transport *via* the plant-type ferredoxin PetF [5,6]. Several trials to implement and optimize an [FeFe]-hydrogenase-based photohydrogen metabolism in cyanobacteria emulating the example of *C. reinhardtii* have been made [7,8]. Among them, the heterologous expression of a clostridial [FeFe]-hydrogenase in *Synechococcus elongatus* sp. 7942 and its coupling to Photosystem 1 (PS1) *via* Fd of the host was most successful [9]. While photohydrogen evolution clearly exceeded the H_2-production activity of the native [NiFe]-hydrogenase, it did not reach the level of anaerobic *C. reinhardtii* cultures. This is

Abbreviations: *C. reinhardtii*, *Chlamydomonas reinhardtii*; Fd, PetF, ferredoxin; FNR, ferredoxin-NADP$^+$-reductase; HydA1, [FeFe]-hydrogenase of *Chlamydomonas reinhardtii*; *S.* 6803, *Synechocystis* PCC 6803; PS1, Photosystem 1

* Corresponding author.
E-mail address: matthias.roegner@rub.de (M. Rögner).
[1] Authors contributed equally.

https://doi.org/10.1016/j.bbabio.2018.01.006
Received 5 September 2017; Received in revised form 18 January 2018; Accepted 22 January 2018
Available online 31 January 2018

possibly due to insufficient enzyme maturation and the rather low compatibility of the heterologous clostridial HYDA to the electron mediator PetF (Fd) of the host cell. A major reason is the complex structure of clostridial [FeFe]-hydrogenase that requires the synthesis of four additional [FeS]-clusters besides the active center cofactor (H-cluster) and that also has not been evolved to interact with plant-type ferredoxins. Both problems could be solved by using an algal-type [FeFe]-hydrogenase such as HydA1 of *C. reinhardtii* that requires only H-cluster maturation and is directly connected to the photosynthetic electron transfer (PET) through PetF [10]. Photohydrogen production is also limited by redox enzymes competing with [FeFe]-hydrogenase for electrons from Fd – especially ferredoxin-NADP-oxidoreductase (FNR). In *C. reinhardtii* a knock-down of FNR expression caused a 2.5-fold increase of photohydrogen production under sulphur-deprivation [11] which is explained by the K_M of Fd for FNR being approximately by a factor of 10 lower than for HydA1 [5,6].

For this reason, manipulation of the electron flow at the acceptor side of PS1 that funnels about 90% of the reducing equivalents *via* Fd and FNR into CO_2 fixation is a decisive step for light driven hydrogen production in a cyanobacterial "design cell" [12]. It requires a more detailed understanding about the interactions between reduced ferredoxin and both competing redox partners, *i.e.* FNR and HydA1, on the molecular level, followed by their modifications: Specific weakening of the affinity between Fd and FNR will minimize the activity of the Calvin-Benson cycle and redirect electrons to HydA1. As the extend, up to which percentage electrons can be re-routed without serious effects on the whole cell survival, is unknown, various FNR- and Fd-mutants are necessary in order to be able to fine-tune this manipulation and achieve maximal rates of hydrogen production from a stable phototrophic culture. Although a similar strategy has already been applied for the respective homologs of *C. reinhardtii* [13], cyanobacterial systems are attractive as they are much easier to manipulate genetically and have a much simpler metabolism.

Generally, redox interactions between separate proteins are realized by transient, non-covalently bound complexes [14]. Batie and Kamin [15,16] reported the first FNR mediated electron transfer from Fd to $NADP^+$/NADPH, with Fd interacting in a 1:1 complex with FNR [17]. In this complex electron tunneling is ensured by the close proximity of their two prosthetic groups [18,19]. For the Fd/FNR complex of *Z. mays*, a distance of 6 Å has been determined between the [2Fe-2S] cluster of Fd and FAD of FNR [19]. Also, structural analysis reveals predominantly basic areas on the FNR- and acidic areas on the Fd-surface within their corresponding binding sites. This indicates that the transient interaction between Fd and FNR is mainly driven and guided by electrostatic forces [20]. The same principle applies for the complex formation between ferredoxin and HydA1, resulting in a large overlap of the Fd interaction surface areas for HydA1 and FNR [21]. This was also determined in a nuclear magnetic resonance (NMR) titration experiment with *C. reinhardtii* proteins comparing the effects of HydA1 and FNR titration on the ^1H-^{15}N-HSQC spectrum of ^{15}N-labeled PetF [13].

Synechocystis ferredoxin (Fed1, PetF) is an 11 kDa soluble, acidic protein with strongly negative redox potential (E_m: −412 mV; [22]) and contains a [2Fe-2S] cluster switching between oxidized Fe^{3+}-Fe^{3+} and reduced Fe^{3+}-Fe^{2+} state [23,24]. It is involved in both, cyclic and linear photosynthetic electron flow.

The current study evaluates the impact of single exchange variants of Fd and FNR from *Synechocystis* on their protein-protein interaction and on the partition of reduced Fd for FNR and HydA1, respectively. Positions for FNR-mutants have been selected on basis of the Fd/FNR complex structure from *Z. mays* [19] and analysis of their Fd-dependent enzyme kinetics. Also, five Fd variants have been generated based on a thorough NMR analysis of the Fd/FNR/HydA1 interaction profiles. All mutants have been evaluated in an *in vitro* competition assay between FNR and HydA1 which yields valuable information for design principles of protein-protein interaction and for the construction of a future hydrogen producing cyanobacterial design cell.

2. Material and methods

2.1. Design of expression constructs of ferredoxin

Plasmid constructs for the expression of *Synechocystis* ferredoxin-(*petF*)-variants in *Escherichia coli* were generated based on the vector pASK-IBA7 (IBA-GmbH in Göttingen, Germany). Primers AGTGTAGCT AGCTATACCGTTAAATTGATCACCCCCGATGG and ATGGTAGGTCTCA TATCAGTAAGGTCTTCTTCTTTGTGGG were used to amplify *petF* from genomic DNA isolated from the *Synechocystis* sp. PCC 6803 culture. The amplicon was cloned into pASK-IBA7 *via* restriction sites *Nhe*I and *Bsa*I thereby excising the DNA region which encodes the Strep-tag II peptide. The resulting construct pASK-petF was used as template for site-directed mutagenesis using Phusion High Fidelity DNA-Polymerase (Thermo Fisher Scientific) yielding *petF* variants D22A, D61A, D67A and E71A. Oligonucleotides used for each individual site directed mutagenesis are listed in Table S2.

2.2. Protein expression and purification

Due to the fact that no substantial catalytic differences were observed between the long and the short form of FNR – FNR_L and FNR_S, respectively (see Fig. S4), all experiments have been performed with FNR_S, which will be designated FNR hereafter (in case of FNR *wild type*: FNR-WT).

For the heterologous overexpression of FNR variants or FNR_L in *E. coli* strain BL21 (DE3) the His_6-tagged *petH* gene of *Synechocystis* sp. PCC 6803 (slr1643) was subcloned into the expression vector pASK-IBA37+ (IBA-Lifesciences, Goettingen, Germany) yielding plasmid IBA37-petH. The expression construct was also used as template for site directed mutagenesis using Phusion High Fidelity DNA-Polymerase (Thermo Fisher Scientific) yielding *petH* variants D71K, K75A/D and K78A/D. Primers for *petH* gene amplification and mutagenesis primers are listed in Table S2. The expression culture (8 × 500 ml) was inoculated with 10 ml of a 100 ml LB pre-culture grown over night from a single colony and cultivated under constant shaking (180 rpm) at 37 °C up to an OD_{578} of 0.6. FNR expression was induced during the following 6 h of continuous cultivation by the addition of Anhydrotetracycline (AHT) up to 0.2 µg/ml. Cells were harvested by centrifugation at 4 °C (20 min, 15,900 g), followed by snap freezing of the pellet with liquid nitrogen and storage at −20 °C until further use. *E. coli* cell disruption was achieved by passing the resuspended pellet at 4 °C 7-times through a French press (1000 psi) (SLM Amico French Pressure Cell Press). For protein purification an immobilized metal ion affinity chromatography (IMAC) with 5 ml HisTrap crude FF (GE Healthcare) using an ÄKTA purifier 100 (GE Healthcare) exploiting the presence of an N-terminal His_6-tag was combined with a hydrophobic interaction chromatography (HIC) (10 ml Toyopearl Butyl-650 M gravity flow column, Tosoh). FNR was obtained in 50 mM Tris/HCl pH 7.5, 100 mM NaCl buffer (for the activity assays) or in 50 mM potassium phosphate pH 6.8, 50 mM NaCl buffer (for NMR titration experiments) and stored at −80 °C.

E. coli BL21 (DE3) Δ*iscR* was used as host strain for the heterologous expression of both, [FeFe]-hydrogenase HydA1 and Fd variants.

Due to the deletion of the gene encoding *isc*-repressor ISCR this strain provides an elevated [FeS]-cluster biosynthesis backgound to ensure the cofactor coverage of overexpressed [FeS]-proteins [25]. For Fd-expression 2 liter-flasks containing 500 ml VB-medium [26] supplemented with 100 µg/ml ampicillin, 50 µg/ml kanamycin and 4% glucose were inoculated with 20 ml LB preculture (300 ml LB with 0.1% glucose including both antibiotics).

For the expression of ^{15}N-labeled Fd, $Na(NH_4)HPO_4$ of the VB-medium was substituted for Na_2HPO_4 and $^{15}NH_4Cl$ (1.787 g/l VB medium) was added after autoclaving. Also, the preculture was washed with ^{15}N-VB Medium (10 min, 3838 g, 12 °C) and further cultivated for

30 min. Thereafter, 10 ml preculture was used to inoculate 500 ml ^{15}N-VB-Medium (including glucose and antibiotics).

Fd expression was induced (at OD578 = 0.5) by adding 0.2 μg/ml AHT and cultivation was extended to 6 h at 37 °C (160 rpm). Cells were harvested (centrifugation 20 min, 15,900 g, 4 °C) followed by mechanical lysis *via* French press (SLM Amico French Pressure Cell Press). After centrifugation of the lysate (20 min at 39190 g, 4 °C), the supernatant was precipitated twice by ammonium sulphate (45% and 60%) on ice followed by centrifugation (30 min. at 34950 g, 4 °C) and dialysis of the supernatant (Membra-Cel® dialysis tubing, MWCO 7 kDa; SERVA Electrophoresis) overnight in buffer A (20 mM Tricin/NaOH, pH 7.8). The lysat was filtered (0.2 μm), diluted with buffer A and loaded onto a DEAE-Toyopearl-column (30 ml Toyopearl DEAE-650 M, Tosoh) using an ÄKTA purifier 100 (GE Healthcare). Fd-samples, eluted by a linear NaCl-gradient (0% to 70% buffer B, *i.e.* buffer A with 1 M NaCl) were pooled and further purified on a gravity flow Q-Sepharose column (5 ml, Amersham Pharmacia Biotech) with a NaCl-gradient from 0 to 0.8 M. Samples with an absorption ratio (A_{422}/A_{280}) > 0.3 were pooled, concentrated (Amicon®Ultra Centrifugal Filters Ultracel®-10 kDa, Millipore), resolubilized in buffer C (50 mM Tris/HCl, 100 mM NaCl, pH 7.5) and stored at −80 °C.

HydA1 of *C. reinhardtii* was heterologously overexpressed in the unmaturated preform in *E. coli* strain BL21 Δ*iscR* containing only the [4Fe4S]-cluster, followed by protein purification and reconstitution of the $2Fe_H$ subcluster according to the previously published *in vitro* maturation protocol [27,28].

2.3. Sequence alignments and protein structure modelling

Mapping of conserved amino acids in plant-type ferredoxins of *Synechocystis* (*ssl0020/petF*, *sll1382*, *slr1828* and *slr0150*) was done with the web-based tool CLUSTAL OMEGA [29]. The conservancy level was rated as slightly conserved (.), conserved (..) and strongly conserved (*). A model of *Synechocystis* FNR was generated using the online tool SWISS.MODEL [30], based on structural data from *Synechococcus* PCC 7002 FNR (PDB ID: 2B5O).

2.4. NMR titration

NMR samples contained 100–200 μM ^{15}N-labeled Fd in 50 mM potassium phosphate pH 6.8, 50 mM NaCl and 10% D_2O (v/v). All NMR experiments have been performed at 298 K on a Bruker AVANCE 600 spectrometer equipped with a cryogenic probehead. Spectra analysis was done with NMRPipe/NMRDraw [31] and Sparky (T. D. Goddard and D. G. Kneller, University of California, San Francisco).

The assignment of the amide backbone resonances in the 2D ^{1}H-^{15}N-TROSY-HSQC experiment is adapted from BMRB entry 16,024 [32] (Table S1). Potentially participating residues on the Fd side during complex formation with the different FNR-variants and HydA1 (containing the [4Fe-4S] cluster) were identified by recording a series of 2D ^{1}H-^{15}N-TROSY-HSQC spectra [33] of ^{15}N-labeled Fd with binding partner at increasing molar ratios. Weighted averages of the ^{1}H and ^{15}N backbone chemical shift changes Δδ of a particular residue were calculated according to the equation $\Delta\delta = [(\Delta\delta_H{}^2 + 0.2\Delta\delta_N{}^2) / 2]^{1/2}$ with the chemical shift changes for the proton and nitrogen frequency indicated as $\Delta\delta_H$ and $\Delta\delta_N$, respectively [34].

2.5. $NADP^+$ photoreduction assay

Effects of mutagenesis in FNR and Fd on the FNR/Fd complex formation have been evaluated by determining the kinetics of $NADP^+$ photoreduction with 5 mM sodium ascorbate as sacrificial electron donor, combined with 600 μM 2,6-Dichlorophenolindophenol (DCPIP) and 4 μM Cytochrome c_6 (from *T. elongatus*) as electron mediators, PS1 (also from *T. elongatus*) as photosensitizer (10 μg Chl ml^{-1}), Fd as alternative electron mediator and FNR (WT or mutants, 500 nM) as electron acceptor (in 40 μl Tricine/NaOH buffer, 20 mM, supplemented by 10 mM $MgCl_2$ and 0.03% w/v n-Dodecyl β-D-maltoside) (see also Fig. S2). The reaction volume was light exposed (4300 μmol m^{-2} s^{-2}) and vigorously mixed for 5 min (200 rpm) at 25 °C while the reaction kinetics was monitored spectroscopically at 340 nm, following NADPH generation after adding 1 mM $NADP^+$ as substrate. In order to plot the Fd-dependency of FNR activity, the assay was performed under increasing Fd-concentration (0.25, 0.5, 1, 2, 3.5 and 5 μM).

2.6. Light-triggered competition assay

Effects of targeted amino acid exchanges in the binding interfaces of FNR and Fd on the interaction partner preference of Fd were tested *in vitro* by applying the competition assay for H_2 photoproduction acc. to Rumpel et al. [13]. In this study, HydA1 from *C. reinhardtii* was assayed together with wild type and mutagenesis variants of Fd and FNR originating from *Synechocystis* sp. PCC 6803. Instead of PS1, the artificial dye molecule acridine-3,6-diamine (proflavine) was used as photosensitizer which enabled a significantly increased H_2 production volume, as higher effective photosensitizer concentrations can be used. Light-dependent H_2 production was first determined in the absence of a competitor using 100 mM KPO_4, 40 mM EDTA, 3 mM $NaNO_3$, 200 μM proflavin, 10 μM Fd and 50 nM HydA1 in a 200 μl reaction mix (see Fig. S5). The 2 ml reaction tubes were sealed with suba seal stoppers and purged for 5 min with argon before being light exposed (photon radiance: 200 μmol m^{-2} s^{-2}) in a shaking water bath for 30 min at 30 °C. The H_2 production yield was determined in a 400 μl head space *via* gas chromatography (GC-2010, Shimadzu). For the competition assay the control assay reaction mix was supplemented by 2 mM $NADP^+$, 0.36 U NAR and 50 nM of FNR-WT or selected variants. The obtained values have been compared with the respective control sample values without FNR.

3. Results

Despite their wide distribution, Fd and FNR show a high level of evolutionary conservation throughout all oxygenic phototrophs. Especially in case of Fd this largely includes those parts of the surface area which are responsible for the redox partner interaction: In higher plants, Fd and FNR are each present as distinct isoproteins in leaf and root for photosynthesis and heterotrophic metabolism. According to the crystal structures of both types of Fd/FNR complex from *Z. mays* and mutational studies of various charged residues widely distributed on the interface of both complexes, the area around leaf FNR-K88 and -K91 (homologous to cyanobacterial FNR-K75 and -K78, respectively) was shown to be a critical region governing the electrostatic interaction with acidic Fd-residues [35]. We therefore chose K75 and K78 in addition to D71 as targets for site directed mutagenesis in FNR of *Synechocystis* sp. PCC 6803. Notably, K88 and K91 in leaf FNR are substituted to non-charged residues in root FNR, *i.e.* they at least partly contribute to the isotype specific interaction of Fd/FNR and may constitute a fine tuning site for the Fd/FNR interaction. We therefore assumed that similar interaction patterns govern Fd/FNR complex formation in cyanobacteria, green algae and higher plants and used these sites as blue print for the design of our own FNR-mutants.

Also on the basis of evolutionary conservation, D22 and D61 of Fd have been chosen as first targets for mutagenesis in Fd of *Synechocystis* sp. PCC 6803. These positions correspond to D19 and D58 of Fd from *C. reinhardtii* and have been shown to be effective targets for redirecting light induced electron flow from FNR to HydA1 in the homogeneous system of algal proteins [13].

3.1. Characterization of structural Fd-FNR/-HydA1 interaction: interfaces

In order to identify additional target sites on the surface of Fd for the optimization of the electron supply to HydA1 within the

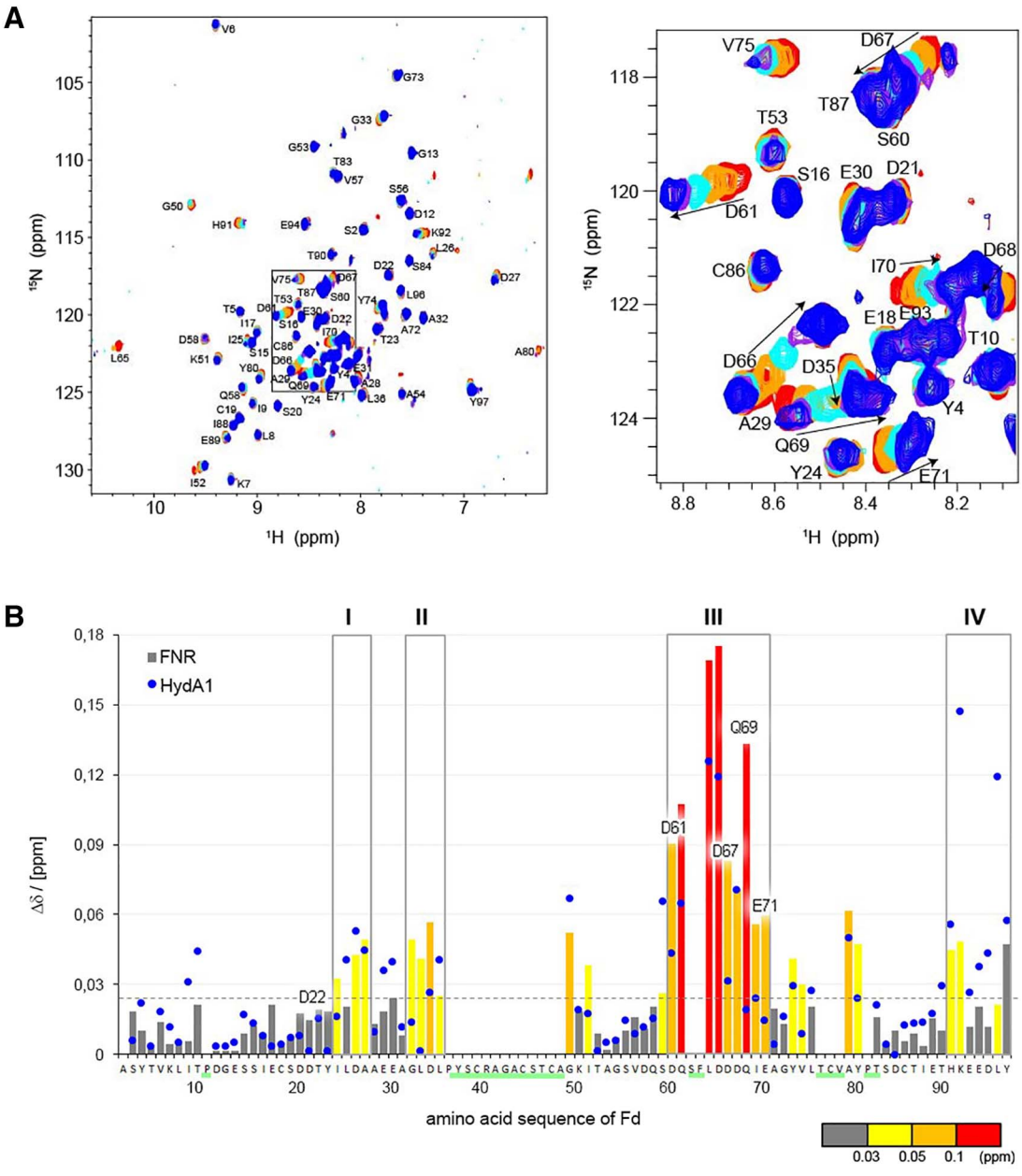

(caption on next page)

Fig. 1. Identification of potential mutagenesis positions in Fd *via* NMR titration with FNR and HydA1. A: ^{15}N,^{1}H TROSY-HSQC spectra of ^{15}N-Fd recorded at 298 K and 600 MHz. Overlay of the spectra in the absence of FNR (red), and for Fd:FNR-ratios of 1:0.02 (orange), 1:0.05 (cyan), 1:1 (violet) and 1:2 (blue). B: Comparison of chemical shift perturbations and interaction surface mappings for Fd upon complex formation with FNR and HydA1. Backbone amide chemical shift changes of ^{15}N-labeled Fd upon adding a 2-fold excess of FNR (bars) and a 6-fold excess of HydA1 (blue circles). Interacting regions indicated by grey squares correspond to the following residues: region I (I25-A28), region II (G33-L36), region III (D61-E71) and region IV (H91-Y97). The broken grey line indicates the resolution limit of 0.025 ppm. C–D: Chemical shift changes mapped onto the 3D surface of Fd_{syn} for FNR- (**C**) and HydA1-binding (D). Amino acid positions were colored corresponding to the chemical shift changes acc. to the following code: Yellow 0.025–0.05 ppm, orange 0.05–0.1 ppm and red > 0.1 ppm. *Residues marked by asterisk have been chosen for site directed mutagenesis.

cyanobacterial design cell, we titrated FNR of *Synechocystis* or HydA1 of *C. reinhardtii* into ^{15}N-labeled Fd and followed binding using ^{1}H-^{15}N TROSY-HSQC spectra. The combined chemical shift changes (Δδ) of the ^{15}N-Fd amide backbone upon binding to FNR were monitored by NMR experiments (Fig. 1A), with the interface of Fd interacting with FNR being classified into four major regions: Region I residues 25–28, region II residues 33–36, region III residues 61–71 and region IV residues 91–97 (see Fig. 1B). These four regions correspond to the hydrophilic and acidic patches surrounding the cluster-binding loops and match very well with the interaction interfaces identified for ferredoxin and nitrite reductase [36], ferredoxin-thioredoxin reductase [37], hydrogenase [38] and FNR from different organisms [14,19]. The cluster binding loops are invisible due to the paramagnetic effect of the [2Fe-2S] cluster.

Overall, the Fd residues affected by HydA1 binding are very similar to the residues affected by FNR-binding (see Fig. 1). However, there are several differences: While I25 and G33, the first residues of region I and II, do not shift significantly upon HydA1 binding, chemical shift changes of E30 and E31 between regions I and II exceed the threshold value of 0.025 ppm. For region III, significant effects already start with S60 (instead of D61) and end with D68 for HydA1 (instead of E71). Remarkably, significant chemical shift perturbations of Fd-region IV upon addition of HydA1 start at T89 and are about twice as large as for FNR. This indicates that the C-terminus of Fd is especially crucial for the interaction with HydA1.

Interestingly, Fd-D61 is one of the few polypeptide positions for which Δδ reaches a value of 0.09 ppm upon titration with FNR, *i.e.* more than twice the value achieved in the titration with HydA1. Similar results were reported for the homologous position in PetF of *C. reinhardtii* - D58 – when titrated with FNR [13]. The exchange Fd-D58A resulted in a 2-fold higher H_2-production rate with HydA1 in presence of FNR. In case of Fd-D22, the effect of the corresponding mutant of the green algal system - Fd-D19A - could not be observed, with both Δδ values being < 0.03 ppm. Instead, the presented HSQC spectra suggest a decreasing binding affinity of Fd to FNR when targeting positions Fd-D35 and Fd-E71. Their chemical shifts are significantly affected by FNR-, but not by HydA1-addition and non-conservative exchanges such as Fd-D35A and Fd-E71A would diminish the negative surface charge for electrostatic attraction and intermolecular salt bridge contacts. In addition, larger chemical shift perturbations have been determined for several other residues of Fd upon FNR-binding when compared to HydA1-binding. Based on the conservancy level of these amino acids as criterion, three additional targets have been selected for site directed mutagenesis: Fd-D67, -Q69 and -E71. Sequence conservancy was determined by aligning the polypeptide sequences of the four Fd isoforms from *Synechocystis* sp. PCC 6803, with the three selected positions representing non-conserved residues to achieve enzyme specificity without causing unwanted cross effects (see Fig. S6).

3.2. Characterization of functional Fd-FNR/-HydA1 interaction: effects of targeted exchanges on activity and HydA1/FNR competition

Site directed mutagenesis variants of both proteins have been characterized concerning their Fd-dependent FNR activity by a PS1-based $NADP^+$ photoreduction assay [39]. Fig. 2 shows the reduction rates for various FNR- and Fd-variants in dependence of the Fd-concentration: While V_{max} of FNR-variants D71K, K75A, K75D and K78A decreases slightly to 78–89% of FNR-WT activity (Fig. 2A), a strong decrease (down to 33% of WT) is observed for FNR-K78D. In case of the Fd-variants, V_{max} decreases for Fd-D61A, while being similar to WT for Fd-D22A; both results are in agreement with the HSQC-experiment.

The effect of the targeted amino acid exchanges was also evaluated by an *in vitro* H_2-photoproduction assay in competition with hydrogenase from *C. reinhardtii* [13] (see Fig. 3). Depending on the affinity of Fd for HydA1 and FNR, respectively, Fd is either oxidized by HydA1 resulting in H_2 production or by FNR resulting in $NADP^+$ reduction. Additionally, $NADP^+$ is recycled in the assay by addition of nitrate reductase and its substrate $NaNO_3$, enabling an unlimited potential for $NADP^+$ photoreduction. In the presence of equimolar amounts of competitive FNR-WT, the H_2 photoproduction rate of HydA1 is reduced to 2–4%. This rate increases to about 30% in presence of FNR-mutant K78D. As other FNR variants resulted in lower H_2 production rates (*i.e.* ≤5% of the standard rate), they have not been considered for the second optimization stage which focused on Fd-variants D22A, D61A, D67A, Q69A and E71A as pre-selected by NMR spectroscopy [13].

The impact of these Fd variants on H_2-photoproduction activity was tested in competitive equilibrium assays with HydA1 and either FNR-WT or FNR variant K78D, respectively. In the absence of FNR, the H_2-photoproduction detected for the different Fd variants was between 82 and 123% of the WT control demonstrating that the chosen Fd-mutations, as expected according to the NMR titration with HydA1, had no severe influence on the Fd-HydA1 interaction (Fig. 4A). Addition of FNR-WT reduced the H_2-photoproduction rate to < 4%, *i.e.* about half of the activity achieved with the corresponding *C. reinhardtii* proteins [13], while variations of Fd's interaction surface area had only a low impact on the interaction with FNR-WT (Fig. 4B). However, these differences were more pronounced when FNR-variant K78D was used as HydA1 competitor (Fig. 4B).

While NMR titration experiments of Fd-WT with FNR-WT show for position Q69 distinctly larger chemical shift difference compared to the titration with HYDA1 (Fig. 1B), there is no significant increase in the H_2-photoproduction activity with Fd-Q69A in the competition assay with either FNR-WT or FNR-K78D. In contrast, other Fd-mutants resulted in increased activity: D22A (+6%), E71A (+15%), D67A (+17%) and D61A (+27%) when assayed with FNR-K78D (Fig. 4B). While the slight positive effect of D22A was unexpected, the impact of the other mutations on H_2 production activity is reflected by the extent of the chemical shift difference in the NMR titrations with FNR (compare bars in Fig. 1B to activity levels in Fig. 4). This confirms the potential of comparative NMR titration experiments for a reliable prediction of selective recognition profiles. In case of Fd-D22A there is only a slight impact on the competition between HydA1 and FNR (Fig. 4B); in contrast, Fd-D61A shows the most prominent effect of all examined Fd variants with FNR-K78D, achieving 73% of the activity measured for the control sample without FNR.

Finally we investigated the competition effects of different FNR variants in combination with the most effective Fd variant, Fd-D61A. However, only double mutants of FNR-K75D/A and FNR-K78D resulted in further enhancements in photohydrogen evolution in comparison with FNR-K78D and Fd-WT (see Fig. S8). Especially variations at position FNR-K75 (see Fig. 3) increased the H_2-production (add. 5–12%).

4. Discussion

The ferredoxin-FNR interaction fulfills an essential role in photosynthetic electron transport, as the affinity of both proteins is decisive

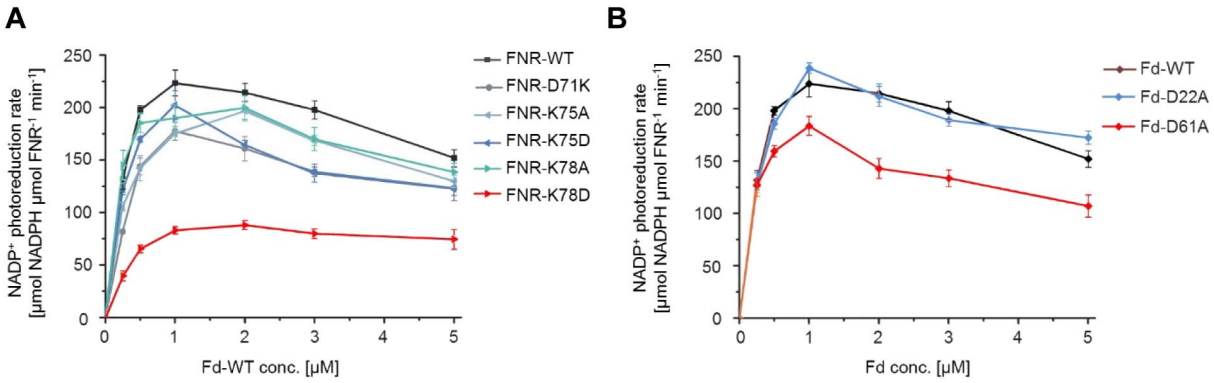

Fig. 2. Analysis of Fd- and FNR-variants by the $NADP^+$ photoreduction assay. A: $NADP^+$-reduction rates of FNR-variants with Fd-WT. **B:** $NADP^+$-reduction rates of Fd-variants with FNR-WT. Error bars indicate the standard deviation of three independent measurements. Error bars represent standard deviations based on two replicates with 3–5 technical repeats.

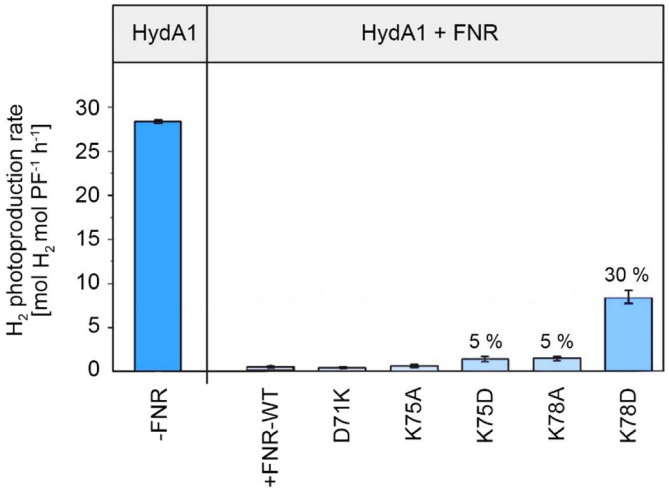

Fig. 3. H_2-photoproduction rate of HydA1 with Fd-WT in competition with different FNR-variants. EDTA was used as sacrificial electron donor, proflavin (PF) as photosensitizer and Fd-WT as electron mediator. (−FNR): Standard *in vitro* assay for light-dependent H_2 production (details see M&M part). (+FNR): Competition assay (details see M&M part) for FNR-WT or selected mutants (*i.e.* D71K, K75A, K75D, K78A, K78D). H_2 photoproduction determined relative to WT control sample (−FNR). Error bars indicate the standard deviation of at least three independent measurements. Error bars represent standard deviations based on two replicates with 3–5 technical repeats.

for the quantity of reducing equivalents provided for C-fixation in competition with other metabolic pathways such as N- and S-fixation, hydrogen production and others. In order to harness photosynthetic electrons for biotechnological products – for instance hydrogen production – the electron flow from Fd to its target proteins has to be engineered by manipulation of Fd-FNR affinities. *In vitro* studies of isolated Fd and FNR from higher plants have shown that both, hydrophobic and electrostatic interprotein forces affect FNR activity and that binding thermodynamics between Fd and FNR are controlled by enthalpy and entropy. These investigations suggested that subtle adjustments in both, hydrophobic and electrostatic forces, are critical for Fd dependent enzymatic activity [40,41]. Focusing on Coulomb forces, studies with Fd, FNR and hydrogenase from green algae have further shown, that hydrogen production in presence of FNR can be effectively shifted by site directed mutagenesis of FNR and Fd [13]. Here we extended these studies towards cyanobacterial Fd and FNR to investigate the potential of protein surface design in combination with hydrogenase HydA1 for the manipulation of electron pathways in a future cyanobacterial design cell. The impact of modified Fd and FNR for the re-routing of electrons can be summarized as shown in Fig. 5.

Details will be discussed separately for Fd and FNR in the following sections.

4.1. Potential impact of Fd for re-routing electrons to H_2ase

Chemical shift perturbations in the HSQC spectrum of ^{15}N labeled Fd upon titration with either HydA1 or FNR could differentiate between polypeptide positions involved in either of the two or both competitive complex formations. A combination of these data with the available crystal structure of the Fd/FNR complex from *Zea mays* and *Anabaena variabilis* [19,42] enabled us to design mutagenesis variants of Fd which result in an enhanced *in vitro* H_2-photoproduction in competition with FNR.

As the risk of affecting the overall protein structure and non-targeted functions is higher when manipulating highly conserved polypeptide positions [43], the online tool CLUSTAL.OMEGA [27] was used to search for non-conserved amino acids among the ferredoxins of *Synechocystis*. From this sub-group, Fd-positions with predicted FNR interaction and low relevance for complex formation with HydA1 (acc. to HSQC-data) have been selected (Fig. 1B, area III), resulting in Q69, D67 and E71, which subsequently were replaced by alanine: Notably, the short aliphatic Ala-side chain cannot be a salt bridge partner nor can it contribute to complex formation *via* H-bond interactions. Deduced from a chemical shift perturbation < 0.045 ppm, the contribution of each selected Fd-position to the Fd/HydA1 interaction is rather small. A comparison of the crystal structure of the Fd/FNR complex from *Z. mays* and the current docking model of apo-HydA1 and PetF from *C. reinhardtii* illustrates the decisive role of Fd surface area III for discriminating between redox partners HydA1 and FNR: While region III effectively contributes to FNR binding it does not seem to be as important for the complex formation with HydA1 (compare region III in both complexes, Fig. 6). In contrast, region IV appears to be much more relevant for interaction with HydA1 than for the Fd/FNR complex formation as suggested by the HSQC results (Fig. 1B).

Remarkably, H_2-photoproduction of HydA1 with cyanobacterial Fd-WT was even more efficient (by 21%) than with the native Fd of *C. reinhardtii*, most probably due to an improved Fd/HydA1 interaction. The additional H_2-photoproduction activity gained by using *Synechocystis* mutants Fd-D22A (+15%) and especially Fd-D61A (+23%) is either similar or significantly higher than the corresponding *C. reinhardtii* variants Fd-D19A (+15%) and Fd-D58A (+3%). For the other tested Fd variants, the Fd/HydA1 interaction is either negatively affected (Fd-D67A; Fd-Q69A) or insignificantly increased (E71A).

Although all tested Fd-variants show only minor effects in competition with equimolar concentrations of FNR-WT, there are distinct differences when FNR-mutant K78D is used as competitor: In this case all Fd-mutants - including Fd-D67A and Fd-Q69A, achieve higher H_2-production rates than Fd-WT. Especially the role of Fd-D61 for interaction partner discrimination is outstanding. This is also reflected by the pronounced differences of the chemical shift perturbations determined upon titration with FNR (0.09 ppm) and HydA1 (< 0.045 ppm) (Fig. 1B).

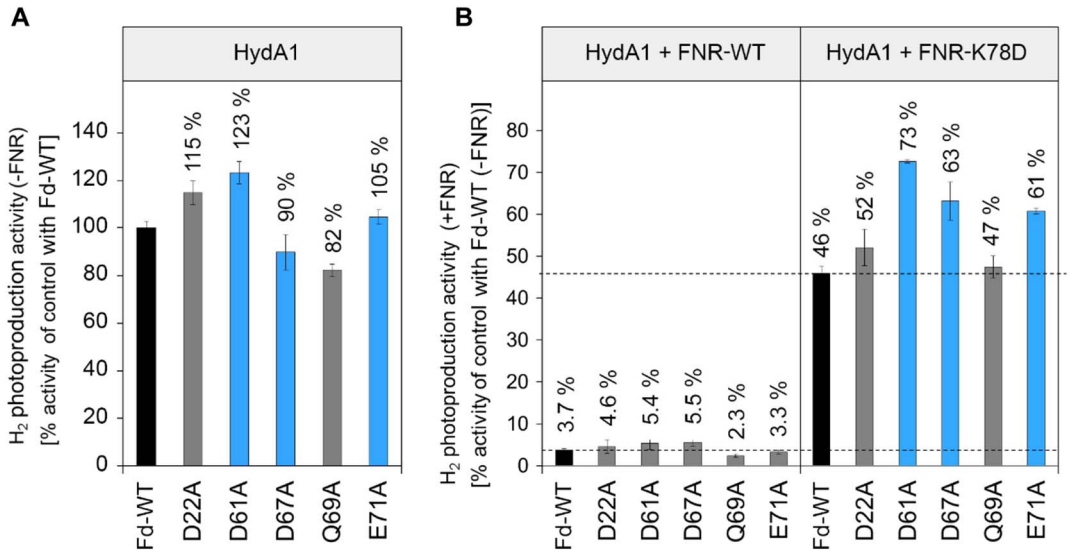

Fig. 4. Impact of Fd-mutants on the H_2 photoproduction rates of HydA1 in presence and absence of FNR-WT or FNR-K78D. A: H_2-photoproduction of HydA1 with six different Fd-species (Fd-WT, D22A, D61A, D67A, Q69A, E71A); standard *in vitro* assay in 100 mM KPO_4 buffer (40 mM EDTA, 3 mM $NaNO_3$, 200 μM proflavin, 10 μM Fd and 50 nM HydA1). B: Competition assay: Standard assay supplemented by 2 mM $NADP^+$, 0.36 U NAR and 50 nM FNR-WT or FNR-K78D. H_2-photoproduction rates relative to WT activity (in A) shown in % above the error bars. Blue bars indicate Fd variants which significantly enhance H_2-photoproduction in presence of FNR. All activities have been normalized to values achieved with Fd-WT and FNR-WT. Error bars represent standard deviations based on two replicates with 3–5 technical repeats.

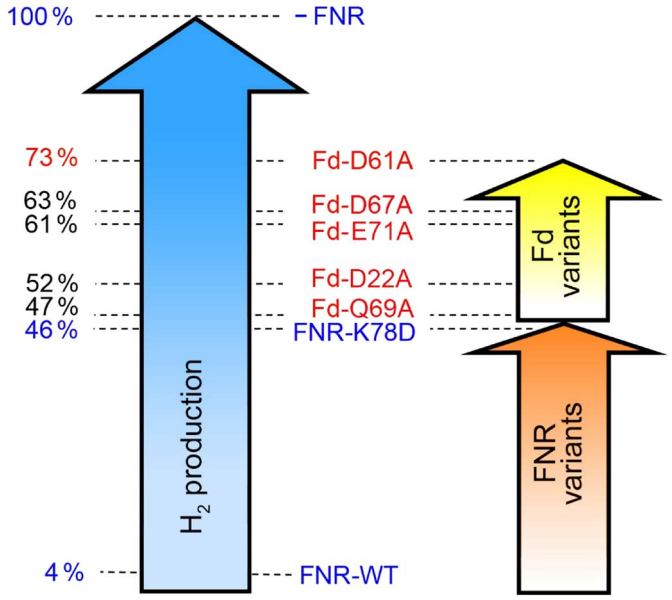

Fig. 5. Impact of cyanobacterial FNR- and Fd-mutants on *in vitro* hydrogen production with HydA1 hydrogenase (*Chlamydomonas reinhardtii*). Competitive conditions with equimolar amounts of FNR and H_2ase.

The HSQC-titration experiments also predicted correctly individual effects of the other amino acid exchanges on the Fd-FNR-complex formation: With the exception of Fd-D22A, distinct negative exchange effects could be expected for all chosen positions. As a matter of fact, the shift difference < 0.02 ppm in titration with FNR correctly suggested for variant Fd-D22A a very low impact on FNR/HydA1 competition. This is in line with the crystal structure of the Fd/FNR complex from *Z. mays* [19] which suggests a localisation of Fd-D22 outside of the complex interface (see Fig. 6). Corresponding exchanges at the homologous amino acids of the *C. reinhardtii* system, *i.e.* Fd-D19A (homologous to Fd-D22A in *Synechocystis*) and Fd-D58A (homologous to D61A in *Synechocystis*) had shown similar tendencies before with D19A exhibiting only a mildly positive effect on H_2 photoproduction in presence of FNR, while D58A had a significantly stronger impact [13]. However, the NMR chemical shift perturbation at Fd-D19 upon Fd/FNR complex formation was clearly higher (0.055 ppm) compared to *Synechocystis*.

The impact of the other exchanges seems to be governed by the type of the targeted amino acid: For instance, the chemical shift perturbation of Fd-Q69 upon titration with FNR is 6–7 times higher than with HydA1, and also considerably higher (> 0.045 ppm) than for all other targeted positions. However, the effect of Fd-Q69A on redox partner selectivity is much lower than for Fd-D61A, Fd-D67A or Fd-E71A. This strong impact of glutamic or aspartic acid may be due to the higher efficiency of salt bridges in complex-formation and -stabilization in comparison to single H-bond partners like glutamine.

In order to confirm that Fd-variants have conserved their native binding compatibility to PS1 we assayed PS1-dependent H_2-photoproduction activity of HydA1 with the most effective variants Fd-D61A and Fd-D67A, reaching 60% and 90% of the control activity determined for Fd-WT (see Fig. S10). The decrease in photo-hydrogen production in case of Fd-D67A corresponds to the behavior of Fd-D19A/D58A from *C. reinhardtii* with the corresponding amino acid exchange (D58A), as it restricted the relative PS1-dependent H_2-evolution yield to about 70% of the activity achieved with Fd-WT [13]. This suggests that the conserved position D61(*Synechocystis*)/D58(*C. reinhardtii*) participates in the complex formation of Fd with the Fd-binding site of PS1, created by the subunits PsaC/-D and -E. However, in case of *C. reinhardtii* the double exchange D19A/D58A still enabled a significantly enhanced H_2-photoproduction in presence of FNR which can also be assumed for Fd-D61A. In case of Fd-D67A, interaction with PS1 is only slightly affected, and as it supports H_2 photoproduction similar to Fd-D61A, Fd-D67A may be even more suitable for PS1-based *in vivo* applications.

In summary, directed mutants of Fd or using Fd from other species can efficiently support the re-routing of electrons towards hydrogen production – in our experiments by up to 27%. We were also able to confirm the high potential of NMR-titration experiments for the evaluation of interaction profiles between ferredoxin and its redox partners [13].

4.2. Potential impact of FNR for re-routing electrons to hydrogenase

Substitutions leading to charge inversion tend to have a stronger effect than a simple charge neutralization as they weaken the general surface charge distribution pattern in addition to the loss of a single salt

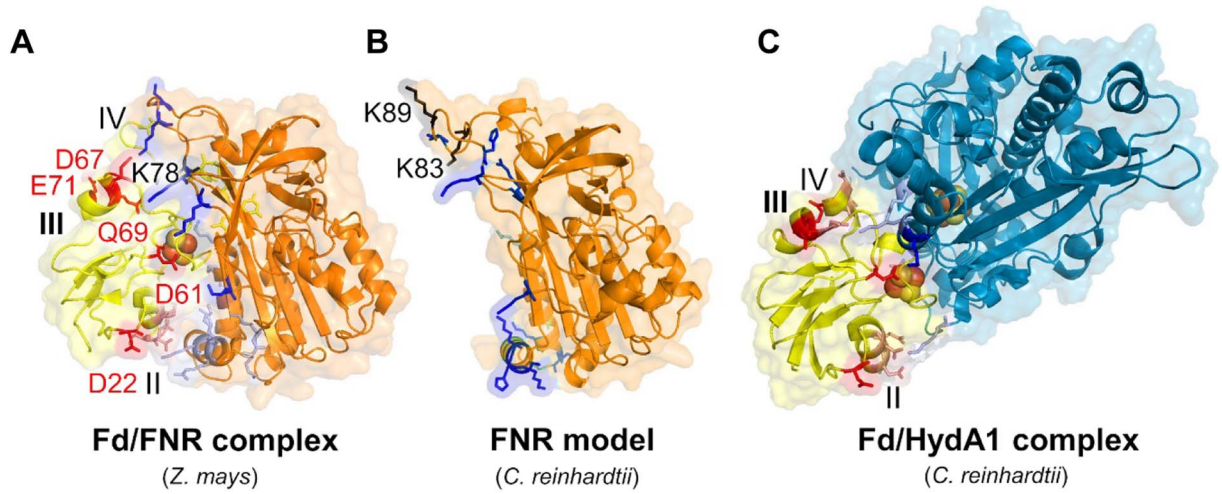

Fig. 6. Surface regions of Fd relevant for the discrimination of the competing redox partners FNR and hydrogenase. A: Maize Fd/FNR complex from leaf (PDB ID: 1GAQ [19]) indicating polypeptide regions II, III and IV of Fd which are critical for discrimination between FNR and HydA1. B: FNR model from *C. reinhardtii*, generated from the FNR crystal structure from *Z. mays* using swiss model (PDB ID: 3LO8) (for details see Fig. S9). C: Model of the Fd/HydA1 complex derived from *in silico* docking, NMR-titration [38] and site directed mutagenesis [5]. Fd in A and C presented as yellow cartoon structure, FNR of *Z. mays* and *C. reinhardtii* (model) in orange and HydA1 of *C. reinhardtii* (PDB ID: 3LX4) in light blue. Major acidic Fd residues chosen for mutagenesis acc. to NMR titrations with both redox partners (Fig. 1) presented as red stick structure. Other potentially involved acidic positions are shown in light red. Basic amino acid residues of FNR and HydA1 are shown as blue (relevant for this study) or grey (less relevant) stick structures. They are participating in complex formation with Fd acc. to previous mutagenesis studies [5], NMR titration (this study and [13]), location within the complex interface in the crystal structure or *in silico* docking complex [38]. FNR-K83 and FNR-K89 from *C. reinhardtii*, which - similar to FNR-K78 (homologous position labeled accordingly in FNR from *Z. mays*) appear to interact with discriminatory Fd-region III, are displayed as black sticks.

bridge partner. In case of FNR-K75 and FNR-K78 (Fig. 3), this is obvious as the exchange to Asp has a significantly stronger impact on the competition between FNR and HydA1. A similar tendency - although less pronounced – is observed for the double exchange variants of FNR (Fig. S8). While the tested Fd variants showed only minor effects on hydrogen production in presence of equimolar amounts of FNR-WT, significant effects, both generally and individually, were observed with mutant FNR-K78D, resulting in a 10-fold increased H_2 production activity relative to Fd-WT and FNR-WT. This is due to a decreased Fd/FNR interaction efficiency as confirmed by the diminished V_{max} of $NADP^+$-photoreduction (by 66%). Experiments with Fd-WT indicated that this FNR variant is by far the most effective in redirecting electrons to HydA1 (Fig. 3). According to the model of the Fd/FNR complex from *Z. mays*, FNR-K78 (homologous to FNR-K91 in *Z. mays*) interacts with acidic residues of region III on the Fd surface, which has already been shown to be crucial for the Fd/FNR complex formation (Fig. 6). Carboxyl group elimination of either Fd-D67 or Fd-D71 results in an additional weakening of this interaction, which explains the significant increase in H_2 photoproduction under competitive conditions by 14–17%.

In case of *Chlamydomonas*, FNR_{Cr}-K89L was the most effective variant which increased the competitive HydA1-based H_2-production from 7 to 18% with Fd-WT [13,44]. However, such a Lys-residue does not exist at the corresponding location in the FNR of *Synechocystis* (see Fig. 6). Probably, a structural loop close to FNR_{Syn}-K78 fulfills this role for the interaction with the cluster of acidic residues on the Fd surface (region III).

In comparison to the *Chlamydomonas* FNR variants, the cyanobacterial FNR-K78D shows a much stronger effect by increasing the competitive H_2-production from 4% with FNR-WT to 46%, *i.e.* by a factor > 10. In combination with the most effective Fd-variant D61A, this activity level can be further increased up to 73%, *i.e.* both mutant proteins show synergistic effects as the 27% increase clearly exceeds the tiny 2% increase achieved with FNR-WT. This is different from the additive effects observed with FNR- and Fd-variants from *C. reinhardtii* [13]. Fig. 6 summarizes our results on the interaction activities of all three partner proteins, *i.e.* Fd, FNR and HydA1 including their variants: It shows specific areas critical for the Fd-FNR interaction (region II: Fd-E31-D35, region III: Fd-D61-A72) and others which are characteristic for Fd-HydA1 interaction (region IV: Fd-T90-L96), combined with the efficiencies of the generated Fd- and FNR-variants. Generally, the impact of contact areas in cyanobacterial systems is similar to the corresponding areas in *Chlamydomonas*, but stronger. Especially re-direction of the electron flow by the cyanobacterial FNR variant (K78D) is significantly stronger (+28%) than in case of *Chlamydomonas*, in which both Fd-mutants and FNR-variants had a similar impact [13].

5. Outlook on future design cell

Experiments reported here show the potential of NMR shift assays in combination with activity assays to predict specific sites of interaction between proteins and how to harness this for re-designing electron pathways. Especially it was shown that rational mutant design is able to overcome an equilibrium between two partner reactions, *i.e.* Fd with FNR (K_m = 2.6–6.6 μM) [44] on the one side and Fd with HydA1 (K_m = 21–35 μM) [5,6] on the other. Using equimolar concentrations of FNR and HydA1, hydrogen production can be increased about 18-fold, directing up to 73% of all photosynthetic electrons towards hydrogen production. Based on these *in vitro* experiments, corresponding Fd and FNR variants are now generated in living cyanobacterial cells (in progress). The outcome of these experiments will tell whether electrons originating from water-splitting can be re-routed at the acceptor side of PS1 under physiological conditions in the designed cell (Fig. 7) to a similar extent as in the *in vitro* assay or whether *in vivo* metabolic constraints suggest the use of less drastic mutants – especially as Fd is electron donor for a large variety of pathways. Also, the oxygen-sensitivity of HydA1 has to be overcome by rational design or directed evolution approaches. Alternatively, oxygen-tolerant hydrogenases have to be engineered for direct interaction with Fd [45]. An alternative strategy would be to develop fusion constructs of PS1 with hydrogenases to minimize the competitive influence of FNR which originates from diffusible Fd, as outlined in [46–48].

Finally, the test of the various mutant species under *in vivo* conditions should indicate the minimal energetic requirement of the photosynthetic cell for survival or – from a biotechnological point of view – the maximal possible harness of photosynthetic electrons for alternative

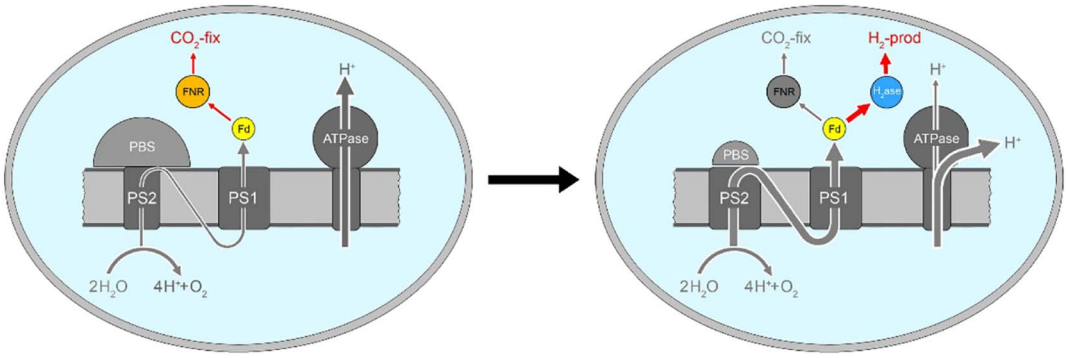

Fig. 7. Future design cell for hydrogen production at the expense of CO_2-fixation. *Re*-routing of photosynthetic electrons from Fd by engineering the binding sites with FNR and HydA1. Besides this, the strategy to increase the amount of photosynthetic electrons for hydrogen production also involves the reduction of phycobilisome antenna size and the partial uncoupling of ATP-synthesis from proton transport as outlined in detail by Rögner 2013.

products such as biofuels.

Transparency document

The http://dx.doi.org/10.1016/j.bbabio.2018.01.006 associated with this article can be found, in online version.

Acknowledgement

The authors would like to thank JF. Siebel for the preparation of apo-HydA1 for the NMR titrations, F. Schulze-Bisping for providing cytochrome c_6, and J. Duan for his contributions for establishing the activity assays. Funding from Deutsche Forschungsgemeinschaft by a DIP grant (Lu 315/17-1, “Nanoengineered optobioelectronics with biomaterials and bioinspired assemblies”) (MR, WL, TH) and from the European Union Seventh Framework Programme for Research, Technological Development and Demonstration under grant agreement No 308518 CyanoFactory (MR) is gratefully acknowledged. This work was further supported by the Federal Ministry of Education and Research, Germany (ERASynBio consortium ‘Sun2Chem’) (BB/M005720/1) (TH) and the Volkswagen Foundation (LigH2t) (Az.: 88240) (TH, MW).

Appendix A. Supplementary data

Supplementary data to this article can be found online at https://doi.org/10.1016/j.bbabio.2018.01.006.

References

[1] C. Wilhelm, T. Jakob, From photons to biomass and biofuels: evaluation of different strategies for the improvement of algal biotechnology based on comparative energy balances, Appl. Microbiol. Biotechnol. 92 (2011) 909–919.
[2] K. Gutekunst, X. Chen, K. Schreiber, U. Kaspar, S. Makam, et al., The bidirectional NiFe-hydrogenase in *Synechocystis* sp. PCC 6803 is reduced by flavodoxin and ferredoxin and is essential under mixotrophic, nitrate-limiting conditions, J. Biol. Chem. 289 (2014) 1930–1937.
[3] A. Melis, T. Happe, Hydrogen production. Green algae as a source of energy, Plant Physiol. 127 (2001) 740–748.
[4] A. Hemschemeier, S. Fouchard, L. Cournac, G. Peltier, T. Happe, Hydrogen production by *Chlamydomonas reinhardtii*: an elaborate interplay of electron sources and sinks, Planta 227 (2008) 397–407.
[5] M. Winkler, S. Kuhlgert, M. Hippler, T. Happe, Characterization of the key step for light-driven hydrogen evolution in green algae, J. Biol. Chem. 284 (2009) 36620–36627.
[6] T. Happe, J.D. Naber, Isolation, characterization and N-terminal amino acid sequence of hydrogenase from the green alga *Chlamydomonas reinhardtii*, Eur. J. Biochem. 214 (1993) 475–481.
[7] Y. Asada, Y. Koike, J. Schnackenberg, M. Miyake, I. Uemura, et al., Heterologous expression of clostridial hydrogenase in the cyanobacterium *Synechococcus* PCC 7942, Biochim. Biophys. Acta 1490 (2000) 269–278.
[8] K. Gartner, S. Lechno-Yossef, A.J. Cornish, C.P. Wolk, E.L. Hegg, Expression of *Shewanella oneidensis* MR-1 [FeFe]-hydrogenase genes in *Anabaena* sp. strain PCC 7120, Appl. Environ. Microbiol. 78 (2012) 8579–8586.
[9] D.C. Ducat, G. Sachdeva, P.A. Silver, Rewiring hydrogenase-dependent redox circuits in cyanobacteria, Proc. Natl. Acad. Sci. U. S. A. 108 (2011) 3941–3946.
[10] S.T. Stripp, T. Happe, How algae produce hydrogen—news from the photosynthetic hydrogenase, Dalton Trans. (2009) 9960–9969.
[11] Y. Sun, M. Chen, H.Y., J. Zhang, T. Kuang, et al., Enhanced H_2 photoproduction by down-regulation of ferredoxin-NADPD reductase (FNR) in the green alga *Chlamydomonas reinhardtii*, Int. J. Hydrog. Energy 38 (2013) 16029–16037.
[12] M. Rögner, Metabolic engineering of cyanobacteria for the production of hydrogen from water, Biochem. Soc. Trans. 41 (2013) 1254–1259.
[13] S. Rumpel, J.F. Siebel, C.F., J.D., E. Reijerse, et al., Enhancing hydrogen production of microalgae by redirecting electrons from photosystem I to hydrogenase, Energy Environ. Sci. 7 (2014) 3296–3301.
[14] P.N. Palma, B. Lagoutte, L. Krippahl, J.J. Moura, F. Guerlesquin, *Synechocystis* ferredoxin/ferredoxin-NADP(+)-reductase/$NADP^+$ complex: structural model obtained by NMR-restrained docking, FEBS Lett. 579 (2005) 4585–4590.
[15] C.J. Batie, H. Kamin, Electron transfer by ferredoxin:$NADP^+$ reductase. Rapid-reaction evidence for participation of a ternary complex, J. Biol. Chem. 259 (1984) 11976–11985.
[16] C.J. Batie, H. Kamin, Ferredoxin:$NADP^+$ oxidoreductase. Equilibria in binary and ternary complexes with $NADP^+$ and ferredoxin, J. Biol. Chem. 259 (1984) 8832–8839.
[17] J.H. Golbeck, Photosystem I: The Light-driven Plastocyanin: Ferredoxin Oxidoreductase, Springer Science & Business Media, 2007.
[18] E.A. Ceccarelli, A.K. Arakaki, N. Cortez, N. Carrillo, Functional plasticity and catalytic efficiency in plant and bacterial ferredoxin-NADP(H) reductases, Biochim. Biophys. Acta 1698 (2004) 155–165.
[19] G. Kurisu, M. Kusunoki, E. Katoh, T. Yamazaki, K. Teshima, et al., Structure of the electron transfer complex between ferredoxin and ferredoxin-NADP(+) reductase, Nat. Struct. Biol. 8 (2001) 117–121.
[20] G.P. Foust, S.G. Mayhew, V. Massey, Complex formation between ferredoxin triphosphopyridine nucleotide reductase and electron transfer proteins, J. Biol. Chem. 244 (1969) 964–970.
[21] M. Winkler, A. Hemschemeier, J. Jacobs, S. Stripp, T. Happe, Multiple ferredoxin isoforms in *Chlamydomonas reinhardtii* – their role under stress conditions and biotechnological implications, Eur. J. Cell Biol. 89 (2010) 998–1004.
[22] H. Bottin, B. Lagoutte, Ferredoxin and flavodoxin from the cyanobacterium *Synechocystis* sp PCC 6803, Biochim. Biophys. Acta 1101 (1992) 48–56.
[23] R. Lill, Function and biogenesis of iron-sulphur proteins, Nature 460 (2009) 831–838.
[24] R. Yan, S. Adinolfi, A. Pastore, Ferredoxin, in conjunction with NADPH and ferredoxin-NADP reductase, transfers electrons to the IscS/IscU complex to promote iron-sulfur cluster assembly, Biochim. Biophys. Acta 1854 (2015) 1113–1117.
[25] M.K. Akhtar, P.R. Jones, Deletion of iscR stimulates recombinant clostridial Fe-Fe hydrogenase activity and H2-accumulation in *Escherichia coli* BL21(DE3), Appl. Microbiol. Biotechnol. 78 (2008) 853–862.
[26] H.J. Vogel, D.M. Bonner, Acetylornithinase of *Escherichia coli*: partial purification and some properties, J. Biol. Chem. 218 (1956) 97–106.
[27] G. Berggren, A. Adamska, C. Lambertz, T.R. Simmons, J. Esselborn, et al., Biomimetic assembly and activation of [FeFe]-hydrogenases, Nature 499 (2013) 66–69.
[28] J. Esselborn, C. Lambertz, A. Adamska-Venkatesh, T. Simmons, G. Berggren, et al., Spontaneous activation of [FeFe]-hydrogenases by an inorganic [2Fe] active site mimic, Nat. Chem. Biol. 9 (2013) 607–609.
[29] F. Sievers, A. Wilm, D. Dineen, T.J. Gibson, K. Karplus, et al., Fast, scalable generation of high-quality protein multiple sequence alignments using Clustal Omega, Mol. Syst. Biol. 7 (2011) 539.
[30] M. Biasini, S. Bienert, A. Waterhouse, K. Arnold, G. Studer, et al., SWISS-MODEL: modelling protein tertiary and quaternary structure using evolutionary information, Nucleic Acids Res. 42 (2014) W252–258.
[31] F. Delaglio, S. Grzesiek, G.W. Vuister, G. Zhu, J. Pfeifer, et al., NMRPipe: a multidimensional spectral processing system based on UNIX pipes, J. Biomol. NMR 6 (1995) 277–293.
[32] X. Xu, S. Scanu, J.S. Chung, M. Hirasawa, D.B. Knaff, et al., Structural and

functional characterization of the ga-substituted ferredoxin from *Synechocystis* sp. PCC6803, a mimic of the native protein, Biochemistry 49 (2010) 7790–7797.
[33] K. Pervushin, R. Riek, G. Wider, K. Wuthrich, Attenuated T-2 relaxation by mutual cancellation of dipole-dipole coupling and chemical shift anisotropy indicates an avenue to NMR structures of very large biological macromolecules in solution, Proc. Natl. Acad. Sci. U. S. A. 94 (1997) 12366–12371.
[34] D.J. Craik, J.A. Wilce, Studies of protein-ligand interactions by NMR, Methods Mol. Biol. 60 (1997) 195–232.
[35] F. Shinohara, G. Kurisu, G. Hanke, C. Bowsher, T. Hase, et al., Structural basis for the isotype-specific interactions of ferredoxin and ferredoxin: $NADP^+$ oxidoreductase: an evolutionary switch between photosynthetic and heterotrophic assimilation, Photosynth. Res. 134 (3) (2017) 281–289.
[36] Y. Sakakibara, H. Kimura, A. Iwamura, T. Saitoh, T. Ikegami, et al., A new structural insight into differential interaction of cyanobacterial and plant ferredoxins with nitrite reductase as revealed by NMR and X-ray crystallographic studies, J. Biochem. 151 (2012) 483–492.
[37] X. Xu, S.K. Kim, P. Schurmann, M. Hirasawa, J.N. Tripathy, et al., Ferredoxin/ferredoxin-thioredoxin reductase complex: complete NMR mapping of the interaction site on ferredoxin by gallium substitution, FEBS Lett. 580 (2006) 6714–6720.
[38] S. Rumpel, J.F. Siebel, M. Diallo, C. Fares, E.J. Reijerse, et al., Structural insight into the complex of ferredoxin and [FeFe] hydrogenase from *Chlamydomonas reinhardtii*, Chembiochem 16 (2015) 1663–1669.
[39] J. Jacobs, S. Pudollek, A. Hemschemeier, T. Happe, A novel, anaerobically induced ferredoxin in *Chlamydomonas reinhardtii*, FEBS Lett. 583 (2009) 325–329.
[40] M. Kinoshita, J.Y. Kim, S. Kume, Y. Sakakibara, T. Sugiki, et al., Physicochemical nature of interfaces controlling ferredoxin NADP(+) reductase activity through its interprotein interactions with ferredoxin, Biochim. Biophys. Acta 1847 (2015) 1200–1211.
[41] M. Kinoshita, J.Y. Kim, S. Kume, Y. Lin, K.H. Mok, et al., Energetic basis on interactions between ferredoxin and ferredoxin $NADP^+$ reductase at varying physiological conditions, Biochem. Biophys. Res. Commun. 482 (2017) 909–915.
[42] R. Morales, M.H. Charon, G. Kachalova, L. Serre, M. Medina, et al., A redox-dependent interaction between two electron-transfer partners involved in photosynthesis, EMBO Rep. 1 (2000) 271–276.
[43] M.J. Betts, R.B. Russell, Amino-acid Properties and Consequences of Substitutions. Bioinformatics for Geneticists, John Wiley & Sons, Ltd, 2007, pp. 311–342.
[44] A. Decottignies, Alternative end-joining mechanisms: a historical perspective, Front. Genet. 4 (2013) 48.
[45] O. Lenz, L. Lauterbach, S. Frielingsdorf, B. Friedrich, Oxygen-tolerant hydrogenases and their biotechnological potential, in: M. Rögner (Ed.), Biohydrogen, de Gruyter, Berlin, 2015, pp. 61–96.
[46] S. Rexroth, K. Wiegand, M. Rögner, Cyanobacterial design cell for the production of hydrogen from water, in: M. Rögner (Ed.), Biohydrogen, de Gruyter, Berlin, 2015, pp. 1–18.
[47] C.E. Lubner, A.M. Applegate, J.H. Golbeck, Re-routing redox chains for directed photocatalysis, in: M. Rögner (Ed.), Biohydrogen, de Gruyter, Berlin, 2015, pp. 239–264.
[48] M. Ihara, H. Nishihara, K.S. Yoon, O. Lenz, B. Friedrich, et al., Light-driven hydrogen production by a hybrid complex of a [NiFe]-hydrogenase and the cyanobacterial photosystem I, Photochem. Photobiol. 82 (2006) 676–682.